

**NOTICE**

This report was prepared as an account of work sponsored by the United States Government. Neither the United States nor the United States Energy Research and Development Administration, nor any of their employees, nor any of their contractors, subcontractors, or their employees, makes any warranty, express or implied, or assumes any legal liability or responsibility for the accuracy, completeness, or usefulness of any information, apparatus, product, or process disclosed, or represents that its use would not infringe privately owned rights.

## NEUTRON SCATTERING STUDIES OF ELECTRON-PHONON INTERACTIONS

**MASTER**

J.D. Axe

Institute Laue-Langevin, Grenoble, France, and

Brookhaven National Laboratory, Upton, N.Y., U.S.A.

This review is an attempt to summarize the areas in which neutron scattering has been used in studying electron-phonon interactions, and to display some of the key results. The examples chosen reflect the interests of the author and represent in no way a complete survey of the subject.

### I. PHONON DISPERSION IN METALS

The most obvious and direct way in which electron phonon interaction manifests itself is in the phonon dispersion of metals. When phonon dispersion curves of simple metals are analyzed by Born-von Karman theory typically force constants between fifth nearest or even more distant neighbors are needed.<sup>1,2</sup> Furthermore, the magnitude of the successive force constants is often oscillatory,<sup>2,3</sup> reflecting the rather long ranged oscillatory character of electronic screening. Born-von Karman models are both unwieldy and unphysical, and it is now generally recognized that it is more satisfactory to formulate models in which conduction electron-phonon interactions are explicitly dealt with.

In the harmonic approximation phonon frequencies and eigenvectors are obtained by diagonalizing a dynamical matrix  $D(\vec{q})$ . For our purposes a sufficiently general form is<sup>4</sup>

$$D_{xy}(\vec{q}) = \frac{1}{V} \sum_{\vec{G}} \left( (\vec{G} + \vec{q})_x \phi(\vec{G} + \vec{q})(\vec{G} + \vec{q})_y - \vec{G}_x \psi(\vec{G}) \vec{G}_y \right) \dots (1)$$

\*Research carried out, in part, under the auspices of the United States Energy Research and Development Administration under Contract No. EY-76-C-02-0016.

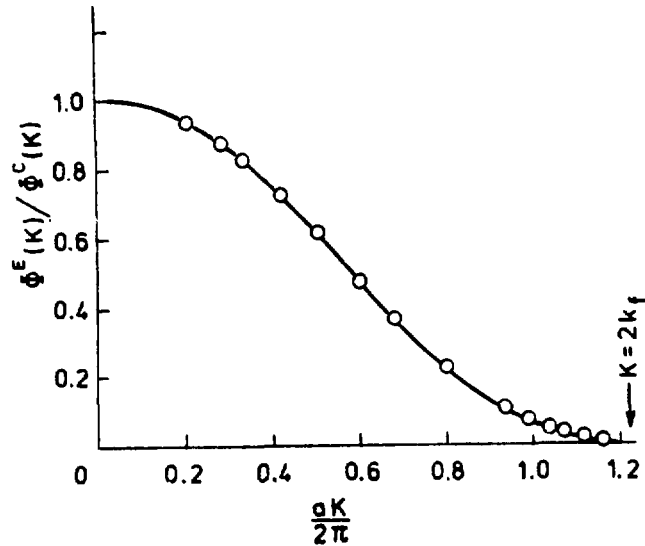


Fig. 1 The effective electron screening potential for sodium metal. The solid curve is deduced from phonon dispersion measurements (Ref. 5). The crosses represent calculations by Toya (Ref. 6).

where  $\phi(\vec{K})$  is the Fourier transform of an appropriate ion pair potential,  $v$  is the volume of a unit cell and the sum is over all reciprocal vectors  $\vec{G}$ . For metals it is convenient to write the potential as the sum of three terms,

$$\phi(\vec{K}) = \phi^C(\vec{K}) + \phi^R(\vec{K}) + \phi^E(\vec{K}) \quad \dots(2)$$

representing a) Coulomb interactions between ions, b) core repulsion of ions and c) ion-electron-ion interactions, respectively.

Figure 1 shows a comparison of the potential for sodium derived by Cochran<sup>5</sup> from experimental phonon dispersion curves,<sup>1</sup> compared with an early calculation by Toya<sup>6</sup> which attempted to deal in a fundamental way with the conduction electrons.  $\phi^E(\mathbf{K})$  is normalized by the coulomb term  $\phi^C(\mathbf{K}) = 4\pi e^2/K^2$ . Although the agreement is remarkably good, the further comparison of the measured

and calculated dispersion curves, while impressive, was not completely satisfactory. This is the result of the near cancellation of the  $\phi^+$  and  $\phi^-$  terms in eq. (2). ( $\phi^+$  is nearly negligible in sodium.) As a result phonon dispersion in metals generally provides a very stringent test of our understanding both of electron-ion potentials and of many body screening effects within the electron gas itself. It is fair to conclude that much of the stimulus for developments in pseudopotential theories<sup>7</sup> over the last decade came with the availability of reliable inelastic neutron scattering measurements of phonons in metals.<sup>8,9</sup>

The additional comment that must be made concerning Figure 1 is that it is not in general possible to uniquely deduce interionic potentials from phonon dispersion curves. There are two distinct difficulties. The first is that both the phonon frequencies and eigenvectors are needed to reconstruct the dynamical matrix  $\tilde{D}(\vec{q})$ . Although the eigenvectors can in very favorable cases be deduced from inelastic scattering intensities, in simple structures the problem is best resolved by measuring along those directions in reciprocal space where the eigenvectors are fixed by symmetry. The second problem is that the structure of eq. (1), which in principle involves reciprocal lattice vectors  $\vec{R}$  of arbitrarily large value, is such that no unique value of  $\tilde{D}(\vec{q})$  can be deduced from a knowledge of  $D(\vec{q})$ . This reflects the fact that in a real space formulation  $\tilde{D}(\vec{q})$  depends only upon  $\partial\phi/\partial r$  and  $\partial^2\phi/\partial r^2$  evaluated at distances of interatomic separation. Cochran was able to derive  $\phi^E(K)$  shown in Figure 1 only by assuming physically plausible constraints on its behavior.

## II. KORN SINGULARITIES

Korn singularities arise because of the abrupt changes in electronic screening which occur when the phonon wavevector  $\vec{q}$ , spans the Fermi surface of a metal.<sup>10</sup> The effect is most simply discussed in the case where the electron wavefunctions are sufficiently plane-wave-like over most of the unit cell to allow  $\phi^E(K)$  to be approximately factorized in the form

$$\phi^E(K) = -[v(K)] \epsilon_0 v(K) / (1 + v_0(K) \chi^0(K)) \quad \dots(3)$$

Here  $v(K)$  is the effective ion-electron potential and  $v_0(K)$  is the electron coulomb plus exchange potential.<sup>11</sup>  $\chi^0(K)$  is the familiar one electron susceptibility

$$\chi^0(\mathbf{k}) = \sum_{\mathbf{k}'} \frac{f_{\mathbf{k}'} - f_{\mathbf{k}'+\mathbf{k}}}{\epsilon_{\mathbf{k}'\mathbf{k}}} \quad \dots(4)$$

The magnitude of the Kohn singularity depends greatly on how well pieces of Fermi surface separated by the wavevector  $\mathbf{k}$  are matched. For simple ellipsoidal surfaces where the matching is poor  $\chi^0(\mathbf{k})$  is regular, but there is a logarithmic singularity in the derivative  $\partial\chi^0(\mathbf{k})/\partial\mathbf{k}$ .<sup>12</sup> Brockhouse, et. al.<sup>13</sup> were the first to find phonon anomalies with these expected properties in a study of lead. Lead is favorable because of the large electron-ion potential,  $v(\mathbf{k})$ . In most other simple metals the effects are too small to be obvious by direct inspection of the dispersion curves. Nevertheless, Stedman and coworkers, by making very careful measurements (0.2% precision) and by examining  $\Delta\omega/\Delta q$  have identified a large number of other anomalies in Al<sup>14</sup> and Cu<sup>15</sup> as well as Pb<sup>13</sup>. (It is important to realize that while the first moment of the line shape can be determined with such precision, the lines typically have a width ~5% due to instrumental resolution.) A substantial fraction of the anomalies have been assigned to known features of the Fermi surface with reasonable certainty. Ng and Brockhouse<sup>17</sup> have followed the changes in the size of the Fermi surface that occurs when Pb is alloyed with Tl.

In the event that a substantial portion of the Fermi surface "nests" into a matching portion displaced by a wavevector  $\mathbf{k}$ , the singularity in  $\chi^0(\mathbf{k})$  becomes stronger. In the limit of perfect nesting there is a logarithmic singularity in  $\chi^0(\mathbf{k})$  rather than in  $\partial\chi^0/\partial\mathbf{k}$ .<sup>12</sup> When the nesting is less than mathematically perfect it is still possible to have strong cusp-like singularities in  $\chi^0(\mathbf{k})$  itself.<sup>12,15</sup> Such cusps are seen in the phonon dispersion in Cr,<sup>13</sup> Mo,<sup>14</sup> and W,<sup>16</sup> and are believed to result from nesting of electron and hole pockets in the rather complex Fermi surfaces of these materials. A particularly strong example occurs in Cr, as shown in Figure 2. Nb and Nb-Mo alloys also have suspected Kohn anomalies at wavevectors that can be reasonably correlated with a rigid band model of the Fermi surface.<sup>14,15</sup> While it is often possible to find qualitative correlations, it is a common observation that anomalies predicted by simple considerations of Fermi surface topology are in some cases too weak to be observed and in other cases relatively strong. There has been little effort to understand the shape and strength of the anomalies in a quantitative way.<sup>18</sup>

It is a very striking fact that many high  $T_c$  superconductors exhibit rather broad anomalous dips in their dispersion relations which are not seen in their neighboring low  $T_c$  counterparts.<sup>19</sup> For example, (Figure 3) Nb has such features which are not seen in Mo, and similar relationships are observed in the V, Cr and Ta, W

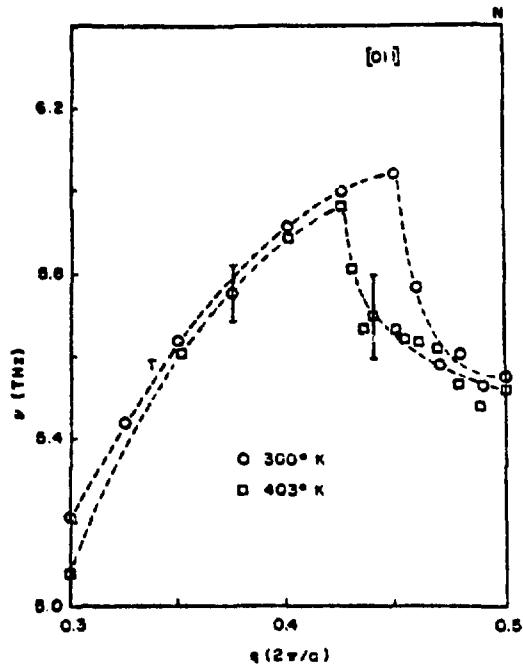


Fig. 2 A portion of the phonon dispersion of chromium near the N symmetry point at two temperatures. (Ref. 19).

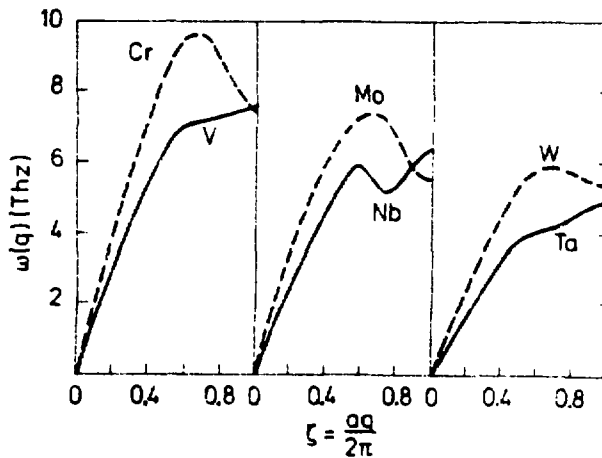


Fig. 3 Longitudinal acoustic phonons in group V and VI transition metals. (After ref. 20).

pairs. Similar features have been pointed out by Smith and his coworkers<sup>11</sup> for the transition metal carbides. These features are too broad to be Kohn anomalies and furthermore, as has been shown for the Nb-Mo system, do not scale with the size of the Fermi surface. Sinha and Harmon<sup>12</sup> have proposed a model in which collective charge fluctuations within the localized d-states softens the lattice response. They suggest that a large density of d-states at the Fermi surface is required. It is not clear whether the correlation with high  $T_c$  superconductivity, which undoubtedly exists, is or is not a causal one.

### III. NEUTRON SPECTROSCOPY OF SUPERCONDUCTORS

Thus far we have been concerned with the electronic screening effects of the phonon frequencies. These can be adequately described in the adiabatic approximation. In order to discuss the influence of the electrons on phonon linewidths, it is necessary to consider the damping due to excitation of electron-hole pairs. This is accomplished by replacing the static susceptibility  $\chi^0(K)$  in eq. (3) by

$$\chi^0(K, \omega + i\eta) = \sum_{\mathbf{k}} \frac{f_{\mathbf{k}} - f_{\mathbf{k}+\mathbf{K}}}{\epsilon_{\mathbf{k}+\mathbf{K}} - \epsilon_{\mathbf{k}} + \omega + i\eta} \quad \dots(5)$$

The electronic damping is introduced via  $\text{Im } \chi^0(K, \omega)$ , and is in most cases small enough to be completely masked by phonon-phonon scattering. In a neutron scattering experiment this in turn is usually masked by instrumental resolution!

Nevertheless in strong coupling superconductors in the vicinity of  $T_c$  there are abrupt changes in electronic damping which are sufficiently strong to be studied by neutron scattering.<sup>26,27</sup> This behavior arises because phonons with energy less than that of the temperature-dependent superconducting energy gap,  $2\Delta(T)$ , are energetically incapable of decaying by excitation of electron-hole quasiparticle pairs.

Although the theory of this effect dates from the early BCS period<sup>28</sup>, the effect was first seen in neutron scattering some ten years later in Nb<sub>3</sub>Sn.<sup>26</sup> Recently more refined measurements have been performed in Nb.<sup>27</sup> Figure 4 summarises some of these latter measurements. When  $2\Delta(T)$  equals the phonon energy,  $\hbar\omega_p$ , an abrupt change occurs in the linewidth. Certain qualitative features, such as the displacement of the curves to lower temperature with increasing phonon energy, are obvious from the sketch included in

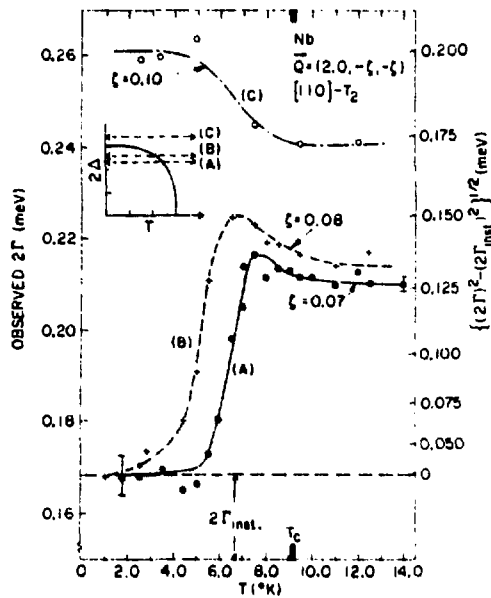


Fig. 4. Temperature dependence of several  $[110]T_2$  phonons in Nb, showing the change in width due to the superconducting gap.

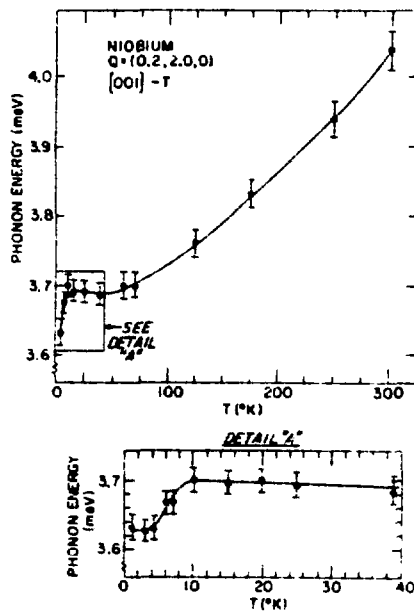


Fig. 5. Temperature dependence of  $[111]T_1$  phonon frequency in Nb.

the Figure. The rounding of the discontinuity can be partly accounted for by resolution effects. All three sets of data in Figure 4 show that when  $\hbar\omega$  slightly exceeds  $2\Delta(T)$  the phonon linewidths are greater than their values far above  $T_c$ . This effect, which is due to an increased density of electron states at the gap energy, is in qualitative agreement with theory. Since the real and imaginary parts of  $\chi^0(K, \omega)$  are related by Kramers-Kronig relations, we expect<sup>29</sup> and find anomalies in the phonon frequencies in the vicinity of  $T_c$  as well (see Figure 5).

Measurements of this type are of course of interest because they provide an alternate means for direct determination of the temperature dependence and anisotropy of the gap energy. In addition, they measure that part of the phonon linewidth,  $\gamma_{ep}$ , which is due to electron-phonon interaction. Allen<sup>30</sup> has pointed out that is very closely related to quantities of interest in strong coupling superconductivity by deriving a simple explicit relation between  $\gamma_{ep}$  and the electron-phonon spectral function  $\alpha^2F(\omega)$ .

Obviously neutron scattering measurements of this sort are successful only if the electron-phonon interaction is sufficiently strong that the quenching of the interaction when  $2\Delta(T) \geq \hbar\omega$  produces a measurable effect. Given presently available spectrometer resolution, the technique is unfortunately restricted to a small handful of strong coupled superconductors.

#### IV. MAGNETIC FIELD EFFECTS

In the preceding section we saw how the presence of an energy gap in the conduction electrons can be manifested in the phonon spectrum. Another way of introducing energy gaps in the conduction electrons is by application of an external magnetic field, and under suitable conditions this too may produce interesting effects in the phonon spectrum.

When a magnetic field is applied to a metal the energies of the conduction electrons are quantized into a series of Landau levels. In momentum space this quantization is represented by the condensation of the electron energy states into a series of tubes, each having a constant cross section in a plane perpendicular to the applied field,  $\vec{H}$ , as shown in Figure 6. The cross sectional area of each tube is proportional to  $\vec{H}$ . The energy of an electron lying on the  $n$ 'th tube is

$$\epsilon_n(k_z) = (n + \frac{1}{2})\hbar\omega_c + \frac{\hbar^2 k_z^2}{2m_{\parallel}}$$

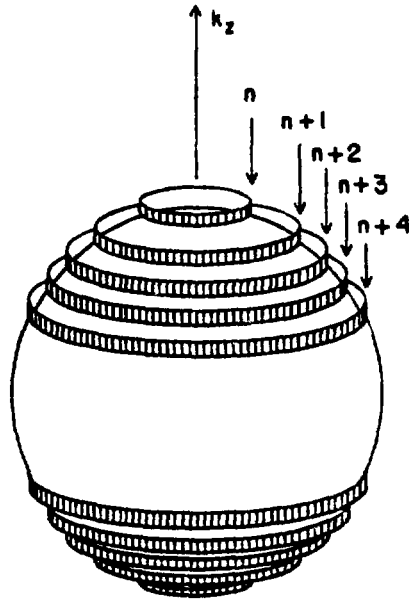


Fig. 6 Free electron Fermi surface and tubes onto which electron states condense in a magnetic field along  $k_z$ . (Ref. 30).

where  $k_{||}$  is the component of the electron wavevector parallel to  $\vec{H}$ ,  $m_{||}$  is an effective mass and  $\omega_c$  is the cyclotron frequency.

In the free electron case, as discussed by Dawley,<sup>31</sup> and by Sham,<sup>32</sup> there are two distinct kinds of effects depending upon whether the phonon propagation vector, is parallel or perpendicular to  $\vec{H}$ . For  $\vec{q} \parallel \vec{H}$  there are Kohn-like singularities in  $\chi^0(q, \omega, H)$  whenever  $q$  equals the length,  $2k_n$ , of the portion of the  $n$ 'th tube that lies within the Fermi surface.<sup>33</sup> However even for low  $H$  there are  $\sim 10^3$  Landau levels below the Fermi energy, so that the tubes are very closely spaced relative to the available momentum resolution of a neutron spectrometer and the strong field induced singularities are greatly smoothed out.

When  $\vec{q} \perp \vec{H}$ ,  $\chi^0(q, \omega, H)$  has a different character reflecting the fact that phonons can now scatter electrons from the  $n$ 'th to the  $(n + p)$ 'th tube, subject to the condition

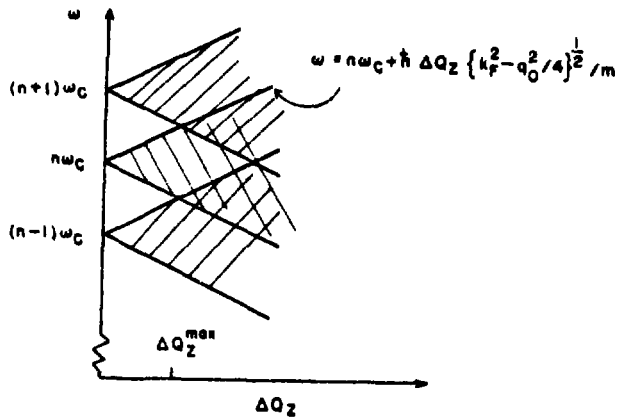


Fig. 7  $\text{Im } \chi(Q, \omega)$  is finite in the shaded area with a magnetic field perpendicular to the phonon propagation. (Ref. 34).

$$\epsilon_{n+p}(k_z) - \epsilon_n(k_z) = p\hbar\omega_c = \hbar\omega_q \quad \dots(7a)$$

and

$$k_{n+p} - k_n = q \quad \dots(7b)$$

where  $\omega$  and  $q$  are the frequency and wavevector of the phonon and  $k_n$  is the component of the electron wavevector  $\perp H$  for the  $n$ 'th tube. This is just the cyclotron resonance condition, and we consequently expect the electron-phonon interaction to contribute to the lifetimes of only those phonons whose frequencies are integral multiples of the cyclotron frequency.

A more detailed consideration of the possibility of observing the effect of a transverse magnetic field on phonon lifetimes by conventional neutron spectroscopy has been given by Fynn and Axe.<sup>34</sup> Figure 7 shows the effect of a small component of phonon wavevector,  $\Delta Q_z$ , parallel to  $\vec{H}$  on the electron quantization of electrons.  $\omega_c = (e\hbar/mc) \approx 1 \text{ meV}$  for  $H = 100 \text{ kG}$ , which is well within the capability of a neutron spectrometer to resolve. The major difficulty that occurs is that typical spectrometer momentum resolution extends well beyond the value  $\Delta Q_z^{\text{max}}$  in this Figure, at least in the

case of free electrons. No anomalous effects can then be observed as the smeared value of  $\text{Im } \chi^0(\mathbf{q}, \omega)$  is the same with and without the applied field.

Pynn and Axe suggested that only if there were flat sections of Fermi surface which could be aligned parallel to  $\hat{H}$  could the momentum resolution be sufficiently relaxed to make a neutron scattering experiment feasible. They tested these ideas by measuring the effect of a 50 kG field on phonons near the  $A_1$  Kohn anomaly in Nb.<sup>25</sup> Instead of measuring the width of the phonons directly, they monitored the peak intensity as a function of  $\hat{H}$  and found a small oscillatory component with a period consistent with the cyclotron mass deduced from deHaas-van Alphen measurements.

It is clear that neutrons are potentially very useful to investigate Fermi surfaces, both through Kohn anomalies and cyclotron resonance effects. A distinct advantage, in principle, is that these studies could be extended to impure metals and alloys, which are difficult to study by conventional methods. Similar remarks pertain to the potential of neutron spectroscopy of superconductors. It is fair to conclude, however, that substantial technical improvements will be necessary to make these techniques broadly useful. Order of magnitude increases in reactor fluxes might go a long way toward affecting the necessary resolution, but this is not a likely short term prospect. Unconventional high resolution spectrometers exist,<sup>35,36</sup> but have not as yet been adapted to phonon spectroscopy. It is sobering to recognize that we will often require simultaneous improvements in energy and momentum resolution.

## 7. CHARGE DENSITY WAVE INSTABILITIES

The charge density wave (CDW) state occurs as the result of a Fermi surface instability, which in the absence of electron phonon coupling would be manifested in a divergent susceptibility,  $\chi^0(\mathbf{q}_{\text{CDW}}) \rightarrow \infty$ , at some critical wavevector. The actual instability is a coupled mode which causes a simultaneous modulation of the electron density as well as a distortion of the lattice, i.e. a structural phase transformation. The neutrons couple to the nuclear distortions only. As might be supposed, simple theories predict that CDW phase transformations are accompanied by a soft phonon mode whose frequency is driven to zero by a "giant" Kohn anomaly.<sup>27</sup> The possibility of such an instability is greatly enhanced in lower dimensional systems because of the possibilities for favorable Fermi surface nesting.

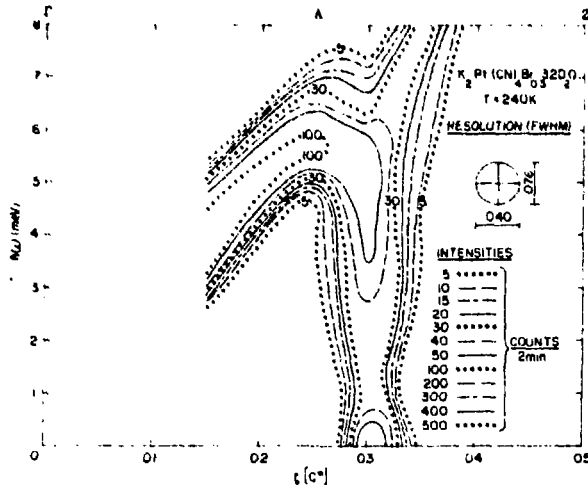


Fig. 3. Inelastic scattering intensity. Contours for KCP showing sharp Kohn anomaly in the acoustic branch near  $\zeta \approx 0.3c^*$  (from Ref. 41).

In the past few years very spectacular examples of giant Kohn anomalies have been studied with neutrons in the quasi-one-dimensional conductors KCP<sup>38-40</sup> and TTF-TCNQ.<sup>41-42</sup> As is demonstrated in Figure 3 the anomaly in KCP is extremely sharp. It occurs whenever  $q_{||}$ , the component of the phonon wavevector along the one-dimensional axis, equals  $2k_F$ . The strength of the anomaly is  $q_{\perp}$  independent of components of momentum perpendicular to the one-dimensional axis. There is a large quasi-elastic central peak revealing the presence of long lived short ranged correlations over a wide range of temperatures, but no actual transition temperature can be defined. It is possible that impurity pinning rather than the effect of one-dimensional fluctuations is responsible for the lack of long range order.<sup>43</sup>

The layered  $d^1$ -metal compounds  $NbX_2$  and  $TaX_2$  ( $X = S, Se, or Te$ ) show a variety of structural transformations<sup>2</sup> which are related to Fermi surface instabilities and CDW formation. Inelastic neutron scattering studies of  $Nb-NbSe_2$  and  $TaSe_2$  show large Kohn-like anomalies in the LA phonons at wavevectors  $Q$  for which Bragg satellite peaks occur at the onset of the CDW state.<sup>44,45</sup> However, the softening of the phonon is incomplete near  $T_C$ , the divergent behavior occurring instead in a quasi-elastic central peak as  $T \rightarrow T_C$ . The Fermi surface geometry is rather complex in these materials and alternative models of Fermi surface nesting have been proposed.

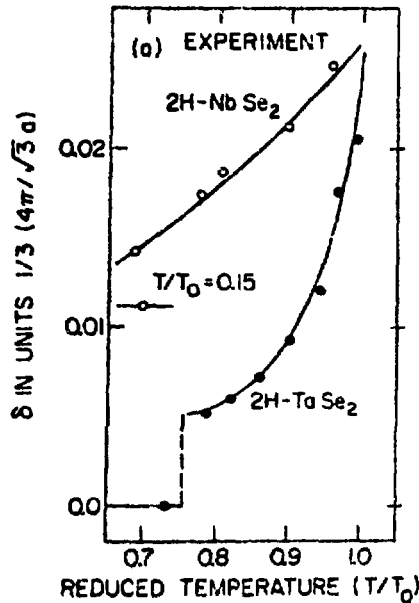


Fig. 9 Temperature dependence of the incommensurate wavevector  $q_0 = (1-\delta)a^*/3$  in  $\text{TaSe}_2$  and  $\text{NbSe}_2$ . A "lock-in" transformation (to  $\zeta = 0$ ) occurs in  $\text{TaSe}_2$  but not  $\text{NbSe}_2$ .

These systems have been extensively reviewed by Wilson, et. al.<sup>46</sup>

One curious feature of CDW transformations is that the wavevector of the modulation,  $q_{\text{CDW}}$ , is in general not an integral sub-multiple of a reciprocal lattice vector of the undistorted parent structure. The resulting structures are termed "incommensurate", and since they lack translational periodicity, they are not strictly speaking crystalline phases. However, the periodic potential of the underlying lattice causes non-integral displacements of the condensed plane-wave displacements and may lead to subsequent transformations which "lock-in" the period of the displacements with that of the lattice. These effects show up clearly in the neutron scattering results<sup>45</sup> on the layered materials shown in Figure 9. The most striking feature is the abrupt change of the satellite wavevector from  $(1-\delta)a^*/3$  to the commensurate value  $a^*/3$  which occurs at  $T \approx 0.7 T_0$ .  $\text{NbSe}_2$  does not achieve the commensurate state even at the lowest attainable temperatures, but as in both the satellite wavevector shows a pronounced temperature dependence, whose origin is closely related to the "lock-in" phenomenon itself. Murton et. al.,<sup>47</sup> using a phonon dispersion theory, showed

that this behavior could be understood by allowing additional secondary distortions with wavevectors chosen to take advantage of the periodic lattice potential. They were also able to directly verify the non-cubic nature of the incommensurate state by observing secondary Bragg satellites at the postulated wavevectors. McMillan<sup>17</sup> and Cox and Emery<sup>18</sup> have recently given more detailed discussions of the nature of the incommensurate ground state.

### References

1. A.D.B. Woods, B.N. Brockhouse, R.H. March, A.T. Stewart and R. Bowers, Phys. Rev. 123, 1112 (1962).
2. B.N. Brockhouse, T. Arase, G. Caglioti, K.R. Rao and A.D.B. Woods, Phys. Rev. 123, 1099 (1962).
3. S.H. Koenig, Phys. Rev. 135A, 1693 (1964).
4. See, for example, W. Cochran and R. Cowley, *Handbuch der Physik*, Vol. XXV/2a, Springer (1967) p. 23 f.f. More generally  $\chi(q)$  is not diagonal in  $q$ , but in simple metals the off-diagonal terms are thought to be small. (L. Sham, Proc. Roy. Soc. A272, 33 (1965)). For simplicity of notation we consider only one atom/cell.
5. W. Cochran, Proc. Roy. Soc. A276, 308 (1963).
6. T. Toya, J. Res. Inst. Catalysis, 6, 191 (1958).
7. See, for example, articles by Heine et al. in "Solid State Physics", Vol. 24, Academic Press (1970).
8. A useful review of the lattice dynamics of metals has been given by S.K. Jooni and A.K. Rajagopal in "Solid State Physics", Vol. 12, Academic Press (1963) p. 159-312.
9. A complete bibliography of neutron scattering results is contained in "Bibliography for Thermal Neutron Scattering", 5th ed., M. Sakamoto, J. Chihara, Y. Nakahara, H. Kadotani, T. Sekiya and Y. Gotan, Japanese Atomic Research Institute, Tokai-mura, Japan.
10. W. Kohn, Phys. Rev. Letters 2, 393 (1959).
11. Perhaps the simplest but by no means only way to arrive at eq. (3) is by pseudopotential methods (see Ref. 2).
12. See L.M. Roth, H.J. Zeiger and T.A. Kaplan, Phys. Rev. 149, 519 (1966).
13. B.N. Brockhouse, T. Arase, G. Caglioti, K.R. Rao and A.D.B. Woods, Phys. Rev. 123, 1099 (1962).
14. J.W. Weymouth and R. Stedman, Phys. Rev. 181, 4743 (1970).
15. G. Nilsson, "Neutron Inelastic Scattering" (International Atomic Energy Agency, Vienna, 1963) p. 187.
16. E. Stellan, L. Almqvist, G. Nilsson and G. Samnio, Phys. Rev. 163, 507 (1967).

17. S.C. Ng and B.N. Brockhouse, "Neutron Inelastic Scattering" (International Atomic Energy Agency, Vienna, 1967) p. 253.
18. T.M. Rice and E.I. Halperin, Phys. Rev. 61, 2903 (1970).
19. M.W. Shaw and L.D. Muhlstain, Phys. Rev. 64, 909 (1971); L.D. Muhlstain, E. Garmen and R.M. Cunningham, "Inelastic Neutron Scattering" (International Atomic Energy Agency, Vienna, 1973) p. 53.
20. S.H. Chen and B.N. Brockhouse, Solid State Commun. 2, 75 (1964). S.H. Chen, Ph.D. Thesis, McMaster Univ. 1964 (unpublished).
21. B.M. Powell, P. Martel and A.D.B. Woods, Phys. Rev. 171, 727 (1968); C.E. Walker and P.A. Egelstaff, *Ibid* 177, 1111 (1969).
22. R.I. Sharpe, J. Phys. C 2, 432 (1969).
23. H.G. Smith, N. Wakabayashi and M. Mostoller in "Superconductivity in d- and f-band metals", B.H. Louglass, ed., Plenum, New York 1976, p. 223.
24. H.G. Smith and W. Gläser, Phys. Rev. Lett. 25, 1611 (1970).
25. S.K. Sinha and B.N. Harmon, Phys. Rev. Lett. 19, 1515 (1972).
26. J.D. Axe and G. Shirane, Phys. Rev. Lett. 31, 218 (1973); Phys. Rev. 68, 1905 (1973).
27. G. Shirane, J.D. Axe and S.M. Shapiro, Solid State Comm. 13, 1893 (1973); S.M. Shapiro, G. Shirane and J.D. Axe, Phys. Rev. B12, 4899 (1975).
28. A. Privorotskii, Sov. Phys. - JETP 1, 948 (1963); V.M. Bobetic, Phys. Rev. A1535 (1964).
29. H.G. Schuster, Solid State Comm. 13, 1559 (1973).
30. P.B. Allen, Phys. Rev. 60, 2577 (1970).
31. R. Cowley, "Neutron Inelastic Scattering" (International Atomic Energy Agency, Vienna, 1967) p. 181.
32. L. Sham, "Modern Solid State Physics", Vol. 2, P.H. Ehm and R.R. Haering, ed., Gordon and Breach, New York, 1969, p. 133.
33. A. Ya Blank and E.A. Kaner, Sov. Phys. - JETP 17, 177 (1963).
34. R. Fynn and J.D. Axe, J. Phys. F 2, 1597 (1972).
35. M. Birr, A. Henzemann and G. Al-Beiruti, Nucl. Inst. Methods 95, 435 (1971).
36. F. Mezel, Z. Physik 206, 146 (1970).
37. S.K. Chan and V. Heine, J. Phys. F 2, 791 (1973).
38. B. Renker, H. Rietsch, L. Pintschovius, W. Gläser, E. Brömm, L. Kuse and M.J. Rice, Phys. Rev. Letters 29, 1106 (1973).
39. K. Carneiro, G. Shirane, S.A. Werner and J. Kwoiler, Phys. Rev. B13, 1258 (1976).
40. R. Comes, B. Renker, L. Pintschovius, R. Carra, W. Gläser and G. Schneider, phys. stat. solidi 171, 177 (1973).
41. H.A. Hook and G.R. Watson, Jr., Phys. Rev. Letters 27, 711 (1971).
42. G. Shirane, S.M. Shapiro, R. Comes, G.R. Watson and A. Heeger, Phys. Rev. B14, 2328 (1976).
43. L.J. Sham and B.N. Patton, "One-dimensional magnetism", H.G. Schuster, -1., Springer-Verlag, New York, 1971.

44. N. Wakabayashi, H.G. Smith and R. Shanks, Phys. Lett. 31A, 307 (1974).
45. D.E. Moncton, G.L. Axe and F.J. DiSalvo, Phys. Rev. Lett. 34, 734 (1975).
46. J.A. Wilson, F.J. DiSalvo and S. Mahajan, Adv. in Phys. 24, 117 (1975).
47. W.L. McDermott, Physical Review B14, 1496 (1976).
48. P. Bak and V.J. Emery, Phys. Rev. Lett. 36, 978 (1976).